ACS Partner Journal

CHEMICAL & BIOMEDICAL IMAGING

pubs.acs.org/ChemBioImaging

Article

Rapid and Large-Scale Synthesis of Chiral and Fluorescent Sulfur Quantum Dots for Intracellular Temperature Monitoring

Li Zhao,[⊥] Tianjian Sha,[⊥] Yufu Liu, Qingsong Mei,* Haibin Li, Pinghua Sun, Haibo Zhou,* and Huaihong Cai*

Cite This: *Chem. Biomed. Imaging* 2024, 2, 817−824

Read Online

ACCESS | Metrics & More | Article Recommendations | Supporting Information

ABSTRACT: The large-scale preparation of fluorescent nanomaterials with laboratory-relevant chemical and optical properties will greatly forward their consumer market applications; however, it still remains challenging. In this work, a universal strategy was developed for the rapid and large-scale synthesis of fluorescent sulfur quantum dots that recently has drawn great attention because of their unique optical characteristics. From the fact that empty 3d orbitals of sulfide species are able to bind with lone-pair π electrons of the heteroatomic groups, many amino-group containing compounds, such as amino acid and polyethylenimine molecules, were exploited to synthesize sulfur quantum dots. This 10 min preparation period endowed sulfur quantum dots with bright blue fluorescence and also chirality. Due to the user-friendly and rapid operation, this strategy can be extended to the large-scale synthesis of sulfur quantum dots with a yield of 16.844 g for one batch of experiment. Moreover, it was found that the sulfur quantum dots exhibited a reversible temperature-dependent luminescent property with a sensitivity of 0.72%/°C, which showed excellent intracellular temperature monitoring capability for inflammation-related disease diagnostics.

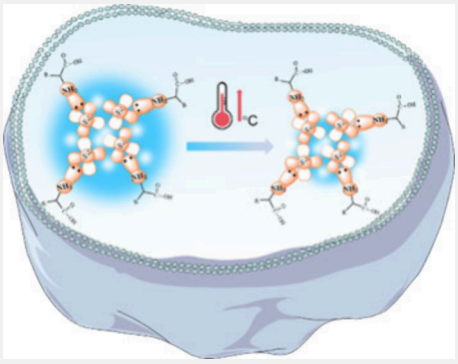

KEYWORDS: *Sulfur Dots, Amino Acid, Fluorescence, Chirality, Cellular Imaging*

INTRODUCTION

Fluorescent nanomaterials including semiconductor quantum dots, carbon dots,[1−6] upconversion nanocrystals,[7−10] and so on, possess widely tunable optical, chemical, and physical properties, enabling them various applications spanning energy harvesting, illumination display, communication and information technology, biology, and medicine.[8,11−19] As novel metal-free quantum dots, sulfur quantum dots (SQDs) recently have been attracting more attention because of their unique features including environmental friendliness, excellent biocompatibility, and tunable surface chemistry.[20−29] However, further progress of SQDs in market-relevant applications requires the development of sustainable and improved preparation strategies with highly reproducible chemical and optical properties.

From the synthetic perspective, the realization of high-quality nanomaterials with large-scale yields based on wet-chemistry synthesis will place increasing attention on reducing the manufacturing costs and preparation time. Recently, a vast number of efforts were devoted to achieve this goal, yet little progress was achieved. SQDs were first reported by Li and co-workers in 2014, which were synthesized via a phase interfacial reaction by CdS quantum dots.[30] Since this initial work, Shen's group prepared the sulfur quantum dots successfully by using sulfur powders with sodium hydroxide and PEG-400 (passivation agent),[31] which was a major breakthrough in sulfur quantum dots preparation. However, the synthesized time of this method is 30−125 h. Wang's group then prepared the precursor by using Shen's method for 5−125 h.[32] After H_2O_2 was injected into the precursor, the surface polysulfide species had been etched to smaller-size sulfur quantum dots. In this method, although H_2O_2 can accelerate the reaction process, the preparation of precursor also expended too much time. Recently, Zhou and co-workers reported an approach for the large-scale synthesis of sulfur quantum dots under a pure oxygen atmosphere,[33] but this method cost 10 h. In order to overcome this time-consuming problem, microwave radiation,[34] hydrothermal method,[35,36] and ultrasonication[37] had been exploited to shorten the reaction time. Moreover, these as-prepared SQDs exhibited good stability, low cytotoxicity, and good cellular uptake, and have been widely used for cellular imaging.[26,38−42] Nevertheless, these methods did not essentially accelerate the reaction process essentially. The rapid and large-scale preparation of sulfur quantum dots still remains challenging.

Received: July 15, 2024
Revised: September 8, 2024
Accepted: September 11, 2024
Published: September 20, 2024

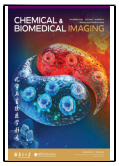

It is well-known that the sublimed sulfur powder can be dissolved in alkaline environment and reacted to become a polysulfide species, such as S^{2-} and S_x^{2-}.[31,32] The empty 3d orbitals of polysulfide species provide a binding site for long-pair π electrons of the heteroatomic groups, such as an amino group or hydroxyl group. Therefore, polysulfide species are able to be well-dispersed with the help of nitrogen- or oxygen-rich ligands.

In this work, a universal strategy for the rapid and large-scale synthesis of fluorescent SQDs was developed based on this knowledge, in which the bright blue emission was obtained through a quick reaction between sublimed sulfur powders, sodium hydroxide, and amino-group containing compounds, such as amino acid or polyethylenimine (PEI) molecules. After the addition of hydrogen peroxide, the polysulfide cluster was rapidly oxidized to SQDs with blue fluorescence under 365 nm UV-light excitation. Moreover, this novel preparation strategy also endowed SQDs with chirality because of the use of chiral amino acids such as cysteine. These preparation processes only need around 10 min in total. Due to the user-friendly and rapid operation, this strategy can be extended to the large-scale synthesis of SQDs, with a yield of 16.844 g for one batch of preparation. Based on the surface-defect-induced luminescence, SQDs are expected to demonstrate a thermosensitive property to monitoring intracellular temperature variations.

EXPERIMENTAL SECTION

Materials

Sodium hydroxide (NaOH, 95.0%), L-cysteine (L-Cys, 99.0%), Dulbecco's Modified Eagle Medium (DMEM), 3-(4,5-dimethylthiazole-2-yl)-2,5-phenyltetrazolium bromide (MTT, 97.0%), 4% paraformaldehyde, and trypsin were obtained from Macklin. Hydrogen peroxide (H_2O_2) and sublimed sulfur (99.5%) were purchased from the Guangzhou Chemical Reagent Factory. Polyethylenimine (PEI, 99%), D-tryptophan (98%), and L-tyrosine (99%) were purchased from Aladdin. Polyethylene glycol-400 (PEG-400) and DL-serine (98%) were purchased from Energy Chemical. Fetal bovine serum (FBS) and antibiotic-antimycotic extracts were obtained from Beyotime.

Instrumentation

UV−visible absorption spectra and PL spectra were measured on a V-730 spectrometer (Jasco Corp., Japan) and a PL FS5 (Edinburgh Instruments, UK) spectrometer. Electronic circular dichroism (CD) spectra were acquired with a Chirascan plus instrument (Applied PhotoPhysics, UK). Fourier transform infrared (FTIR) spectra were recorded on a Nicolet 6700 FTIR spectrometer (Thermo, U.S.). XPS spectra were recorded on a Thermo Scientific K-Alpha$^+$ (ThermoFisher, U.S.). High-resolution transmission electron microscopy (HRTEM) images were obtained using a JEM-F200 transmission electron microscope (JEOL, Japan). Phosphorescence lifetime was measured using an FLS 1000 (Edinburgh Instruments, UK). Confocal laser-scanning microscopy (CLSM) images were recorded on an LSM 880 with AiryScan (Carl Zeiss, Germany) with imaging software ZEN 2.3 (Blue Edition, Carl Zeiss).

Synthesis of Fluorescent Sulfur Quantum Dots

A 2.1 g portion of NaOH and 2.1 g of cysteine were dissolved in 35 mL of water before 0.7 g of sublimed sulfur powder was added. The mixture was stirred at 90 °C for 10 min under atmosphere until sulfur powder dissolved completely. The prepared product was referred to as the precursor, which was a transparent orange solution. Six milliliters of sulfur quantum dots precursor and 4.5 mL of hydrogen peroxide (7.50%) were mixed under vigorous stirring. The color of the mixed solution changed from orange to colorless. Meanwhile, under the 365 nm UV-light illumination, the fluorescence of the solution appeared and gradually became strong, and the product was referred to as "sulfur quantum dots". For purifying the sulfur quantum dots, the product was dialyzed by using a dialysis bag with a molecular weight cutoff of 500 Da for at least 3 days.

Large-Scale Synthesis of Sulfur Quantum Dots

First, 68.4 g of NaOH and 68.4 g of cysteine were dissolved in 1140 mL of water before 22.8 g of sublimed sulfur powder was added. The mixture was stirred at 90 °C for 20 min under atmosphere, until the sulfur powder dissolved completely. The prepared precursor was a transparent orange solution. Next, 1140 mL of sulfur quantum dots precursor and 860 mL of hydrogen peroxide (7.50%) were mixed under vigorous stirring. The mixed solution changed color from orange to colorless under sunlight. Meanwhile, under 365 nm UV-light illumination, the fluorescence of the solution appeared and gradually became strong.

Synthesis of Sulfur Quantum Dots with PEG-400

Four grams of NaOH and 3 mL of PEG-400 were dissolved in 50 mL of water before 1.4 g of sublimed sulfur powder was added as previously reported in the literature.[31] The mixture was stirred at 90 °C for 10 min under atmosphere, until the sulfur power dissolved completely. This mixture solution was named "traditional precursor". A 6 mL portion of the precursor and 4.5 mL of hydrogen peroxide (7.50%) were mixed under vigorous stirring. The solution remained yellow and could not emit fluorescence under 365 nm UV-light illumination.

Synthesis of Sulfur Quantum Dots with Other Amino Acids

First, 0.6 g of NaOH (0.6 g) was dissolved in 10 mL of water, and 0.9060 g of tyrosine, 0.5255 g of serine, and 1.0212 g of tryptophan were respectively added into the above NaOH solution. Next, 0.2 g of sublimed sulfur powder was added into the above mixtures, respectively. These mixtures were stirred at 90 °C under atmosphere until the sulfur powder dissolved completely. The prepared precursors were transparent orange. By dropping the right amount of H_2O_2 into precursors, fluorescent sulfur quantum dots were obtained.

Synthesis of Sulfur Quantum Dots by Polyethylenimine

A 1.05 g portion of NaOH and 4.5 g of PEI were dissolved in 17.5 mL of water. Next, 0.35 g of sublimed sulfur powder was added into the above mixtures. The mixture was stirred at 90 °C under atmosphere until the sulfur powder dissolved completely. The prepared precursors were transparent orange. By dropping 400 μL of 7.50% H_2O_2 into precursors, sulfur quantum dots were obtained.

Cell Culture and MTT Assay

HeLa cells were cultured in Dulbecco's Modified Eagle Medium (DMEM) supplemented with 10% fetal bovine serum (FBS) and 1% antibiotic-antimycotic in an incubator at 37 °C with 5% CO_2. Cell viability was performed using a MTT assay with 3-(4,5-dimethylthiazole-2-yl)-2,5-phenyltetrazolium bromide. HeLa cells were seeded in 96-well plates and incubated for 24 h to reach 80−90%. The medium was replaced by fresh medium containing different concentrations of SQDs with doses of 0, 25, 50, 75, 100, 150, and 200 μg/mL for 24 h. Next, 20 μL of MTT was added into each well of the plate and cultured for 4 h at 37 °C. After the supernatant was removed, 200 μL of DMSO was added into each well to resolve crystal. The absorbance of each well at 490 nm was measured with a microplate reader.

Intracellular Temperature Monitoring

HeLa cells were seeded in a glass bottom cell culture dish for 24 h. Next, cells were incubated with fresh medium containing 40 μg/mL SQDs for 24 h. Afterward, the cells were washed with PBS three times and subsequently fixed with the fresh culture medium to perform fluorescence imaging. Under the confocal fluorescence microscope, the cells were detected three times for each temperature condition.

RESULTS AND DISCUSSION

Sulfur quantum dots herein were rapidly synthesized on a large scale by two steps (Figure 1a). Herein, cysteine as a typical

https://doi.org/10.1021/cbmi.4c00052
Chem. Biomed. Imaging 2024, 2, 817−824

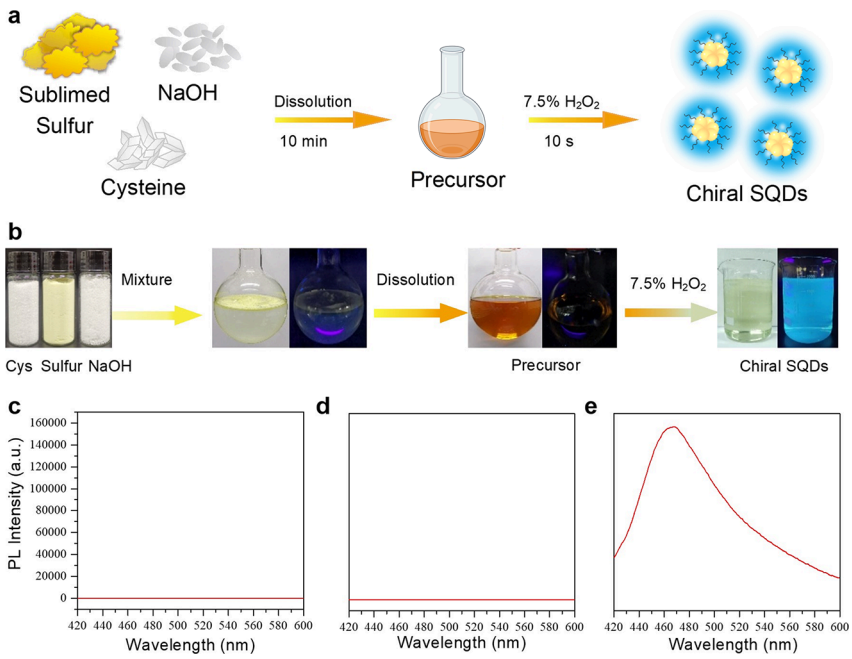

Figure 1. (a) Schematic illustration of the rapid preparation of fluorescent chiral SQDs. (b) Photographic demonstration of the process of large-scale and rapid synthesis of SQDs. Fluorescent spectra of the aqueous solution demonstrated in (b), (c) the mixture solution of reagents, (d) precursor solution, and (e) the obtained SQDs solution.

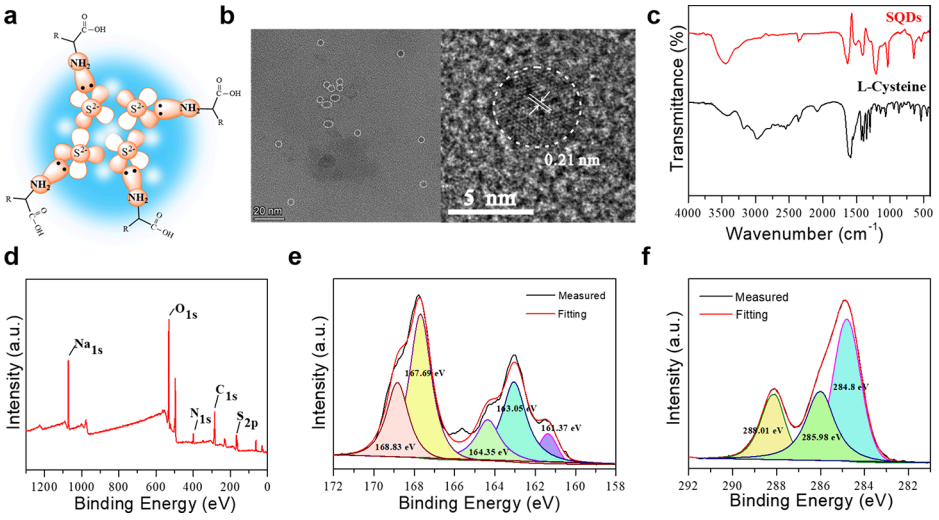

Figure 2. (a) Structural demonstration of sulfur quantum dots. (b) TEM image (left) and HRTEM image (right) of sulfur quantum dots. (c) FTIR spectral comparison of sulfur quantum dots and cysteine. (d) XPS survey spectrum, (e) high-resolution S 2p spectrum, and (f) high-resolution C 1s spectrum of the purified sulfur quantum dots.

lone-pair-electron-containing ligand was taken as an example to demonstrate the preparation strategy. In detail, the mixture of sublimed sulfur powder, L-cysteine, and NaOH was first dissolved in water by vigorously stirring under 90 °C. After the mixture was totally dissolved, the solution color turned from colorless to orange. This process expended about 10 min. By gradually dropping H_2O_2 into the above precursor, the orange-colored solution rapidly turned colorless, and the fluorescent sulfur quantum dots immediately formed in a period of 10 s (Supporting Information videos S1 and S2). However, an amount of precursor identical to that of previously reported methods could not exhibit any observable fluorescence after the addition of H_2O_2 within the same time course (Figure S1). Owing to the rapid and simple preparation process, this novel strategy can be explored in the large-scale synthesis of fluorescent SQDs. As shown in Figure 1b, 22.8 g of sublimed sulfur powder was dissolved in a cysteine alkaline solution. After rapidly reacting with H_2O_2, a large amount of SQDs with a volume of 2 L was obtained with a concentration of 8.4220 mg/mL in one batch of experiment (Figure S2). Moreover, during the synthesis process, both the mixture of reagents and the formed precursor solution did not exhibit any observed fluorescence (Figure 1c and d). After oxidizing by H_2O_2, SQDs were obtained and exhibited bright blue fluorescence with an emission peak at 460 nm under 365 nm UV lamp illumination (Figure 1e).

To reveal the structure of the as-obtained SQDs, a series of structural characterizations were performed. Figure 2a depicts

https://doi.org/10.1021/cbmi.4c00052
Chem. Biomed. Imaging 2024, 2, 817−824

a proposed structural model for SQDs in this work, which consists of S_x^{2-}, S[0], Na_2SO_4, Na_2SO_3, and cysteine. At the center of the sulfur quantum dots, there were polysulfide species around the cysteine molecules. The TEM image in Figure 2b exhibited that the fluorescent sulfur quantum dots remained an inhomogeneous spherical shape with the diameter of 4 nm. The HRTEM image exhibited well-resolved spacing with a clear lattice fringe of 0.21 nm, which was consistent with the reported literature.[33,37,43] The Fourier-transform infrared absorption spectra of purified SQDs displayed obvious peaks at approximately 3800−3300 and 3330−3130 cm^{-1}, which resulted from the stretching vibration of the −OH and $-NH_2$ groups (Figure 2c). The peak at 1663 cm^{-1} was assigned to the stretching vibration of the C═O bonds. The two absorption peaks at 1635 and 1413 cm^{-1} were ascribed to the formation vibration of N−H and C−H.[44] These results indicated that cysteine molecules were conjugated onto SQDs without any structural variations.

The X-ray surface photoelectron spectra (XPS) in Figure 2d demonstrated that the purified SQDs mainly contained C, O, N, and S elements. The high-resolution XPS spectrum of S 2p contained five different peaks (Figure 2e). The peak at 161.37 eV belonged to S_x^{2-}/S^{2-}. Two peaks at 163.05 and 164.35 eV belonged to S[0].[33,45,46] The binding energy peak at 167.69 eV was assigned to SO_3^{2-}.[30,45] The last peak at 168.83 eV was attributed to SO_4^{2-}.[33,47] Furthermore, the high-resolution XPS spectrum of C 1s in Figure 2f exhibited three main peaks. The peaks located at 284.8 and 285.98 eV were attributed to C−C and C═O, respectively, and the binding energy at 288.01 eV was assigned to C−N, C−O, and C−N.[48,49] The high-resolution XPS spectrum of N 1s revealed peaks at 399.05 and 400.99 eV that also indicated the presence of $-NH_2$ and pyrrolic N (Figure S3). Therefore, the sulfur quantum dots consisted of element sulfur, sulfonate groups, and cysteine on the surface, which further verified the proposed structural model in Figure 2a.

The optical characteristics of the obtained sulfur quantum dots were investigated by using the UV−vis absorption spectrum and excitation−emission spectrum. It can be seen from Figure 3a that there is an obvious absorption at 215 nm, which was attributed to n → σ^* transitions.[30,50] On the other hand, there is no distinct absorption peak at 200−250 nm. The sulfur quantum dots can emit a bright blue fluorescence at 460 nm with an excitation wavelength of 370 nm. Interestingly, by adjusting the excitation wavelength from 290 to 450 nm, the emission peaks varied from 380 to 528 nm, with the PL intensity increasing first and then decreasing (Figure 3b). Through more careful study, it had three domain peaks around 380, 460, and 528 nm, which included the near-ultraviolet range and visible region. These results showed the excitation-dependent PL properties in sulfur quantum dots, which were attributed to the inhomogeneous size of the particles. The PL decay curve of the purified sulfur quantum dots in Figure 3c indicated that the emission at 455 nm displayed a lifetime of about 2.77 ns, which is comparable with previously reported SQDs.

Because of the exploration of chiral cysteine as a precursor to the synthesis of SQDs, it is anticipated to endow chirality onto the fluorescent SQDs. The chiral properties of the SQDs were investigated by circular dichroism (CD) spectra (Figure 3d). Interestingly, L-Cys and D-Cys resulted in the generation of L-sulfur quantum dots and D-sulfur quantum dots with almost corresponding mirrored CD spectra (Figures S4 and S5). In

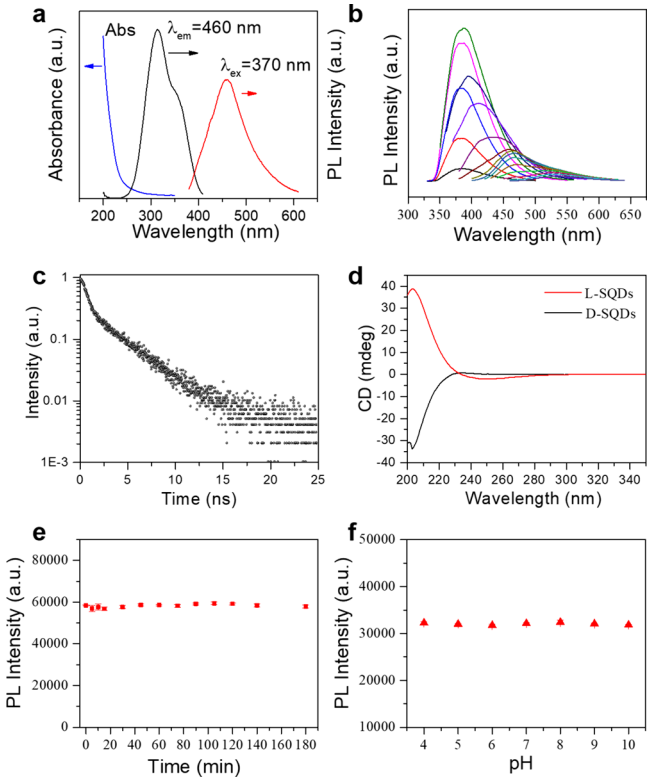

Figure 3. (a) UV−vis absorption spectra, PL spectra (excited at 370 nm), and excitation spectra (emitted at 460 nm) of sulfur quantum dots. (b) PL spectra of sulfur quantum dots taken under different excitation wavelengths. (c) Time-resolved PL spectrum of sulfur quantum dots (excitation and emission wavelengths were set at 340 and 455 nm, respectively). (d) Circular dichroism spectra of the L- and D-sulfur quantum dots. (e) Time stability and (f) pH-dependent photoluminescent intensity of sulfur quantum dots (excited at 370 nm and detected at 460 nm).

order to explore the origin of chirality, the achiral amino acid glycine (Gly) was used to prepare SQDs. It was found that, although the obtained Gly-SQDs exhibited similar fluorescence, the circular dichroism spectra did not show any observable chiral signal (Figure S6). These results indicated that the chirality of fluorescent SQDs should originate from cysteine. This novel property will greatly expand the applications of SQDs, such as chiral recognition, chiral detection, and asymmetric catalysis, avoiding usage of heavy-metal chiral quantum dots.

The fluorescence stability of the as-prepared SQDs toward time and environmental pH is further investigated to demonstrate their practicability. As shown in Figure 3e, the PL intensities of sulfur quantum dots remained unchanged for 3 h, indicating that they had excellent time stability (Figure S7). In addition, the sulfur quantum dots also exhibited good pH-stability in the range 4.0−10.0 (Figures 3f and S8). These results indicated that the rapid synthesis of sulfur quantum dots can obtain stable fluorescence properties.

It is well-known that elemental sulfur could react with sodium hydroxide to form sulfide or polysulfide ions under heating conditions. As Figure 4a shows, sodium hydroxide played an important role in the synthesis of fluorescent sulfur quantum dots. Without the addition of sodium hydroxide, sulfur powder could not be dissolved, and the precursor did not emit any fluorescence. Upon addition of one-half the

https://doi.org/10.1021/cbmi.4c00052
Chem. Biomed. Imaging 2024, 2, 817−824

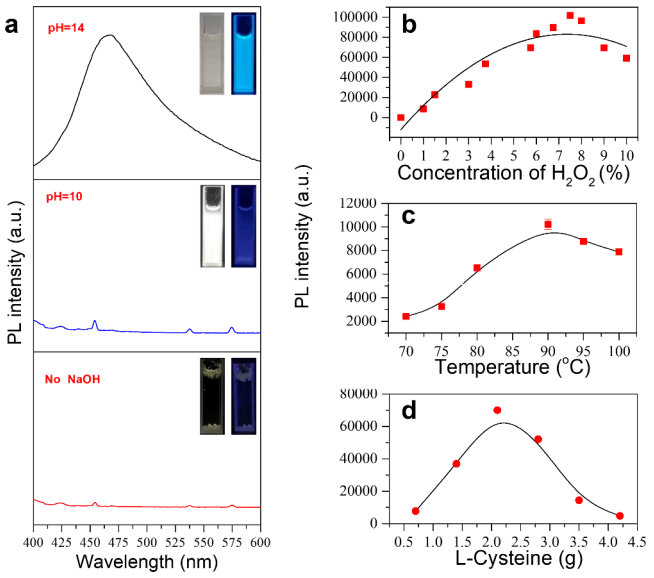

Figure 4. (a) PL spectra of sulfur quantum dots synthesized by three different concentrations of sodium hydroxide and photographs (inset) of sulfur quantum dots in daylight (left) and irradiated by UV light at 365 nm (right). (b) PL intensity (excited at 370 nm and detected at 460 nm) of sulfur quantum dots synthesized using different concentrations of H_2O_2. (c) PL intensity of sulfur quantum dots obtained from the reaction heated to different temperatures, and other conditions: 0.7 g of sublimed sulfur powder, 2.1 g of L-cysteine, 2.1 g of NaOH, and 35 mL of water. (d) PL intensity of sulfur quantum dots obtained from the reaction using different amounts of L-cysteine, and other conditions: 0.7 g of sublimed sulfur powder, 2.1 g of NaOH, 35 mL of water, and 90 °C reaction temperature.

amount of sodium hydroxide, the reactant mixture was dissolved to obtain an orange-colored precursor. However, lots of cysteine was immediately precipitated after the addition of H_2O_2, which should be ascribed to the solution's pH that varied from strong basicity to neutral induced by H_2O_2, and cysteine was oxidized to cystine that greatly decreased its solubility. The resulting solution also was not able to give out any luminescence. After increasing the molar amounts of sodium hydroxide 3-fold to that of sulfur powder, the precursor became stable and could emit bright blue fluorescence after the addition of H_2O_2.

Since sulfion or polysulfide ions are oxidized to SQDs by hydrogen peroxide, increasing the H_2O_2 concentration is believed to raise the photoluminescence intensities of SQDs. It was found that the fluorescence intensity reached a maximum when the concentration of H_2O_2 was 7.5% (Figures 4b and S9). As shown in Figure S10, the absorption of SQDs was decreased by increasing the concentration of H_2O_2. In addition, the synthesizing temperature of the sulfur quantum dot precursor was studied to obtain the optimal fluorescence properties. The photoluminescence intensities of the sulfur quantum dots were recorded at an excitation wavelength of 370 nm. As shown in Figures 4c and S11, 90 °C was the best synthesizing temperature. Furthermore, cysteine played a pivotal role in stabilizing the formed sulfion and polysulfide ions. The results in Figure 4d indicated that both little and high amounts of cysteine led to weak fluorescence (Figures 4d and S12). To demonstrate the universality of this preparation strategy, a few other lone-pair-electron-containing ligands were further used to rapidly synthesize fluorescent SQDs. We also measured the quantum yield of the as-prepared SQDs. The QY was determined by using the reference method with quinine sulfate as a standard reference. The relative quantum yield of as-prepared SQDs is 2.51% (Figure S13 and Table S1). In addition, we designed five different circumstances for sulfur quantum dots synthesis, and we reached the conclusion that the obtained fluorescence SQDs showed excellent stability (Table S2). Herein, tyrosine, serine, tryptophan, and PEI molecules were investigated, where the preparation process was similar to the typical example of cysteine used. As Figure 5

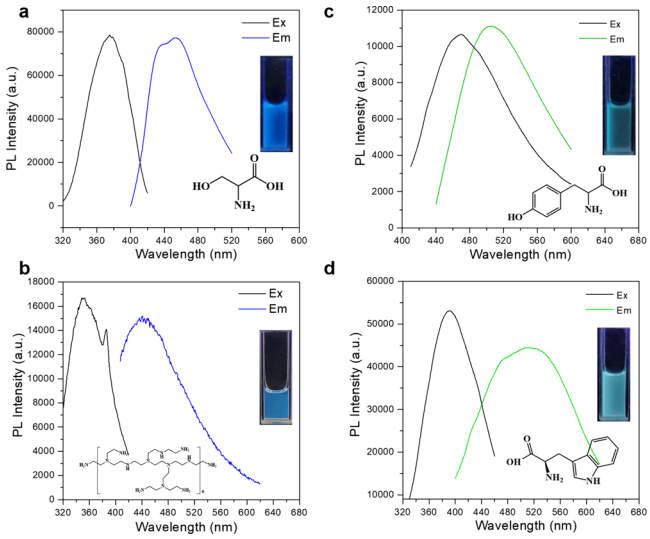

Figure 5. Excitation and emission spectra of sulfur quantum dots synthesized by (a) serine, (b) PEI, (c) tyrosine, and (d) tryptophan. Inset photos are the luminescent photos of these sulfur quantum dots under 365 nm UV light irradiation.

depicts, irrespective of the brightness difference, all of the precursors prepared by these ligands could give out obvious fluorescence upon additions of H_2O_2 without any optimizing synthesis parameters. More interestingly, different from chain-type ligands, such as cysteine, serine, and PEI, SQDs synthesized from aromatic amino acid emitted longer wavelength fluorescence. For instance, tyrosine-based SQDs gave light-green fluorescence under UV lamp illumination, and tryptophan-based SQDs emitted indigo fluorescence (Figure 5c and d). The fluorescence variation may be ascribed to that aromatic π electrons make a contribution to the luminescent process of the polysulfide species.

It is well-known that temperature exhibits a critical role in various physiological activities and intracellular biochemical reactions such as gene expression, cell division, and inflammatory responses. Especially in pathological conditions, the high metabolic activity of cancer cells leads to an increase in temperature. Hence, it is important to achieve sensitive and precise temperature sensing to explore biological processes. Interestingly, the SQDs exhibited a temperature-dependent fluorescence characteristic, and the fluorescence intensity of the SQDs dispersion decreased gradually with rising environmental temperature. The thermoresponsive fluorescence characteristics of SQDs were evaluated in the range of 20–50 °C. Figures 6 and S14 illustrated a substantial decrement on the fluorescence emission with the increase of temperature. Figures 6a and S15 showed the fluorescence intensity decreased within a range of temperature variations between 20 and 50 °C, which should be ascribed to thermos-induced

https://doi.org/10.1021/cbmi.4c00052
Chem. Biomed. Imaging 2024, 2, 817–824

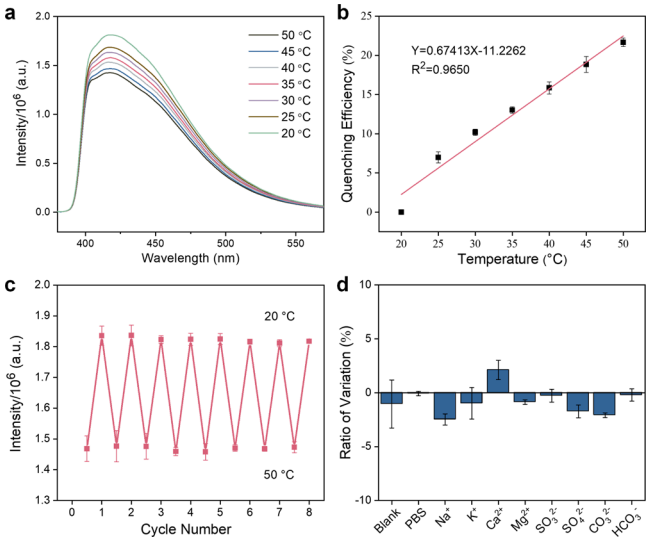

Figure 6. (a) Fluorescence spectra and (b) quenching efficiency of SQDs in water within the range 20−50 °C. (c) The reversibility of the fluorescence for SQDs in response to the variation of temperature by switching back and forth between 20 and 50 °C. (d) Stability of SQDs under different ions conditions.

nonirradiative transition from the surface defects of SQDs. Figure 6b indicated that the quenching efficiency exhibited a linear variation with increasing temperature and presented a linear correlation within 20−50 °C (R^2 = 0.9650). About 21.7% of fluorescent intensity declined within 30 °C temperature variations associated with the sensitivity of 0.72%/°C. This temperature-dependent fluorescence behavior is highly reversible. Figure 6c shows the reversibility of fluorescent response by SQDs to the variation of temperature between 20 and 50 °C. Furthermore, the influence of the intracellular microenvironment on the fluorescence performance of SQDs was evaluated, by focusing on the effect of different ion conditions (Figure 6d). In addition, the SQDs presented a good temperature sensing stability and excitation dependence (Figures S16 and S17). Therefore, SQDs may serve as a suitable nanothermometer for sensing the intracellular temperature.

To demonstrate its intracellular temperature-monitoring capability, the cytotoxicity of SQDs was first investigated by the MTT assay (Figure S18). In brief, the survival rate of HeLa cells remained more than 90% even when the concentration of SQDs reached 75 μg/mL, and remained over 85% at 200 μg/mL after 24 h of incubation. This result indicated its good biocompatibility. The intracellular distribution of the thermoresponsive SQDs was observed by a confocal laser fluorescence microscope with a live cell incubation system, which was used to change the incubation temperature of HeLa cells, and the images are shown in Figure 7a. After incubating for 24 h (40 μg/mL of SQDs), a green fluorescence was observed in cells at different temperature conditions (25−43 °C, Figures S19 and S20). As shown in Figures 7 and S21, the fluorescence intensity of the same cell was found to decrease along with rising intracellular temperature. By measuring the fluorescence intensity (I) of cells at different temperatures (T), a linear calibration was achieved within the range of 25−43 °C, that is, $I = 32.6289 - 0.7313T$ (R^2 = 0.9984) (Figure S22). In addition, the temperature-dependent calibration curve of the fluorescence quenching efficiency in cell (25−43 °C) was depicted in Figure S23. Hence, the above discussions illustrated that SQDs acted as a preferable intracellular nanothermometer, which can be used for disease diagnostics, such as inflammation, infection, and so on.

CONCLUSIONS

In summary, a universal, rapid, and large-scale synthesis strategy for chiral fluorescent SQDs was first developed. With the help of lone-pair-electron-containing groups, stable precursors can be quickly formed and oxidized to SQDs by hydrogen peroxide. This rapid synthesis strategy is further exploited for the gram-scale preparation of SQDs, retaining laboratory optical properties at the same time. Moreover, luminescence color is demonstrated to be adjusted through usage of aromatic-ring-containing ligands, expecting a longer wavelength shifting after further optimizations. This novel SQD demonstrated a sensitive thermos-dependent lumines-

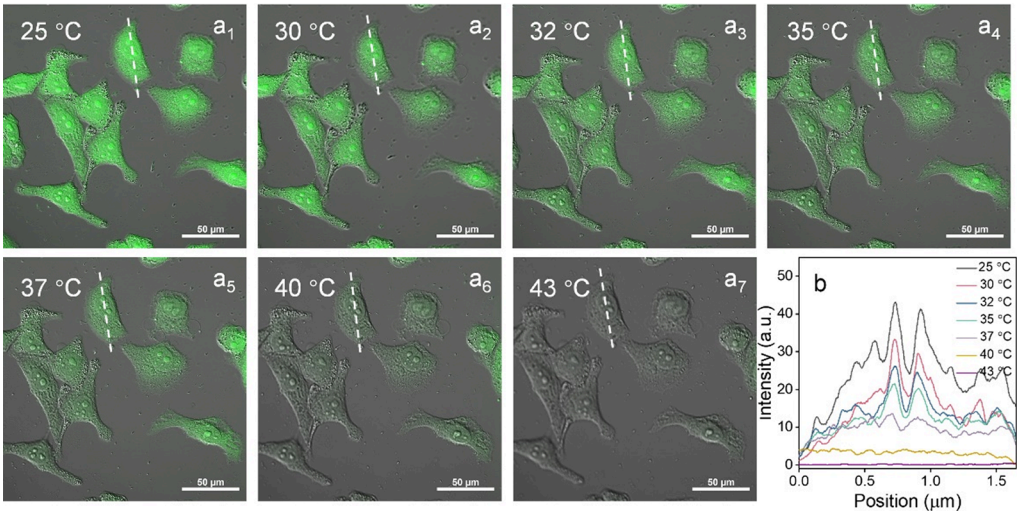

Figure 7. (a) Merge images of HeLa cells (incubated with SQDs for 24 h) obtained in the temperature range of 25−43 °C. The white line demonstrates colocalization of the cell across the seven temperature conditions (25, 30, 32, 35, 37, 40, and 43 °C). (b) The relationship of fluorescence intensity and position of the cell (white line marked) between different temperature conditions (25, 30, 32, 35, 37, 40, and 43 °C).

https://doi.org/10.1021/cbmi.4c00052
Chem. Biomed. Imaging 2024, 2, 817−824

cent intensity and can be used to monitor intracellular temperature variations for disease diagnostics. It is anticipated that this rapid and large-scale synthesis strategy can pave the way for commercial-market applications of SQDs, such as in light-emitting diodes, photocatalysis, solar cells, sensing, and imaging.

■ ASSOCIATED CONTENT

Supporting Information

The Supporting Information is available free of charge at https://pubs.acs.org/doi/10.1021/cbmi.4c00052.

Picture of sulfur quantum dots under UV light; XRD, CD spectra, UV−vis absorption spectra, PL spectra of sulfur quantum dots, and confocal fluorescence images of cells under different temperatures (PDF)

Video S1: Video for rapid preparation under natural light (MP4)

Video S2: Video for rapid preparation under UV light (MP4)

■ AUTHOR INFORMATION

Corresponding Authors

Qingsong Mei − *School of Medicine, Jinan University, Guangzhou, Guangdong 510632, China;* orcid.org/0000-0003-4327-6931; Email: qsmei@jnu.edu.cn

Haibo Zhou − *College of Pharmacy, Jinan University, Guangzhou, Guangdong 510632, China;* orcid.org/0000-0002-0098-5968; Email: haibo.zhou@jnu.edu.cn

Huaihong Cai − *College of Chemistry and Materials Science, Jinan University, Guangzhou, Guangdong 510632, China;* Email: thhcai@jnu.edu.cn

Authors

Li Zhao − *College of Pharmacy, Jinan University, Guangzhou, Guangdong 510632, China*

Tianjian Sha − *College of Pharmacy, Jinan University, Guangzhou, Guangdong 510632, China*

Yufu Liu − *School of Medicine, Jinan University, Guangzhou, Guangdong 510632, China*

Haibin Li − *College of Pharmacy, Jinan University, Guangzhou, Guangdong 510632, China*

Pinghua Sun − *College of Pharmacy, Jinan University, Guangzhou, Guangdong 510632, China; Key Laboratory of Xinjiang Phytomedicine Resource and Utilization, Ministry of Education, School of Pharmacy, Shihezi University, Shihezi, Xinjiang 832003, China*

Complete contact information is available at: https://pubs.acs.org/10.1021/cbmi.4c00052

Author Contributions

⊥L.Z. and T.S. contributed equally to this work.

Notes

The authors declare no competing financial interest.

■ ACKNOWLEDGMENTS

This work is financially supported by the National Natural Science Foundation of China (82373833, 22177039, and 22074028), the National Key Research and Development Program of China (2021YFC2300400), and the Guangdong Basic and Applied Basic Research Foundation (2024A1515012204). We gratefully acknowledge the support of the K. C. Wong Education Foundation. We are very grateful for the testing services provided by the Analysis and Test Center of Jinan University. The computational analysis in this research was supported by the High Performance Public Computing Service Platform of Jinan University.

■ REFERENCES

(1) Chen, L.; Yang, S.; Li, Y.; Liu, Z.; Wang, H.; Zhang, Y.; Qi, K.; Wang, G.; He, P.; Ding, G. Precursor Symmetry Triggered Modulation of Fluorescence Quantum Yield in Graphene Quantum Dots. *Adv. Funct. Mater.* **2024**, *34*, No. 2401246.

(2) Huang, X.; Qin, Y.; Guo, T.; Liu, J.; Hu, Z.; Shang, J.; Li, H.; Deng, G.; Wu, S.; Chen, Y.; Lin, T.; Shen, H.; Ge, J.; Meng, X.; Wang, X.; Chu, J.; Wang, J. Long-Range Hot-Carrier Transport in Topologically Connected HgTe Quantum Dots. *Adv. Sci.* **2024**, *11*, No. 2307396.

(3) Kumar, V. B.; Mirsky, S. K.; Shaked, N. T.; Gazit, E. High Quantum Yield Amino Acid Carbon Quantum Dots with Unparalleled Refractive Index. *ACS Nano* **2024**, *18* (3), 2421−2433.

(4) Llusar, J.; du Fossé, I.; Hens, Z.; Houtepen, A.; Infante, I. Surface Reconstructions in II−VI Quantum Dots. *ACS Nano* **2024**, *18* (2), 1563−1572.

(5) Xu, H.; Song, J.; Zhou, P.; Song, Y.; Xu, J.; Shen, H.; Fang, S.; Gao, Y.; Zuo, Z.; Pina, J. M.; Voznyy, O.; Yang, C.; Hu, Y.; Li, J.; Du, J.; Sargent, E. H.; Fan, F. Dipole−dipole-interaction-assisted self-assembly of quantum dots for highly efficient light-emitting diodes. *Nat. Photonics* **2024**, *18* (2), 186−191.

(6) Zhu, C.; Boehme, S. C.; Feld, L. G.; Moskalenko, A.; Dirin, D. N.; Mahrt, R. F.; Stöferle, T.; Bodnarchuk, M. I.; Efros, A. L.; Sercel, P. C.; Kovalenko, M. V.; Rainò, G. Single-photon superradiance in individual caesium lead halide quantum dots. *Nat.* **2024**, *626* (7999), 535−541.

(7) Feng, Y.; Lei, D.; Zu, B.; Li, J.; Li, Y.; Dou, X. A Self-Accelerating Naphthalimide-Based Probe Coupled with Upconversion Nanoparticles for Ultra-Accurate Tri-Mode Visualization of Hydrogen Peroxide. *Adv. Sci.* **2024**, *11*, No. 2309182.

(8) Feng, H.-J.; Zeng, L.; Li, J.-Y.; Lin, W.-Y.; Qi, F.; Jiang, L.-H.; Zhang, M.-Y.; Zhao, Y.; Huang, L.; Pang, D.-W. Natural Protein Photon Upconversion Supramolecular Assemblies for Background-Free Biosensing. *J. Am. Chem. Soc.* **2024**, *146* (31), 21791−21805.

(9) Song, N.; Fan, X.; Guo, X.; Tang, J.; Li, H.; Tao, R.; Li, F.; Li, J.; Yang, D.; Yao, C.; Liu, P. A DNA/Upconversion Nanoparticle Complex Enables Controlled Co-Delivery of CRISPR-Cas9 and Photodynamic Agents for Synergistic Cancer Therapy. *Adv. Mater.* **2024**, *36* (15), No. 2309534.

(10) Wang, Y.; Rui, J.; Song, H.; Yuan, Z.; Huang, X.; Liu, J.; Zhou, J.; Li, C.; Wang, H.; Wu, S.; Chen, R.; Yang, M.; Gao, Q.; Xie, X.; Xing, X.; Huang, L. Antithermal Quenching Upconversion Luminescence via Suppressed Multiphonon Relaxation in Positive/Negative Thermal Expansion Core/Shell $NaYF_4$:Yb/Ho@ScF_3 Nanoparticles. *J. Am. Chem. Soc.* **2024**, *146* (10), 6530−6535.

(11) Chen, M.; Han, Q.; Zhang, M.; Liu, Y.; Wang, L.; Yang, F.; Li, Q.; Cao, Z.; Fan, C.; Liu, J. Upconversion dual-photosensitizer−expressing bacteria for near-infrared monochromatically excitable synergistic phototherapy. *Sci. Adv.* **2024**, *10*, No. eadk9485.

(12) Dolai, J.; Joshi, P.; Mondal, P. P.; Maity, A.; Mukherjee, B.; Jana, N. R. Blinking Carbon Dots as a Super-resolution Imaging Probe. *ACS Appl. Mater.* **2024**, *16* (13), 16003−16010.

(13) Kim, D. C.; Seung, H.; Yoo, J.; Kim, J.; Song, H. H.; Kim, J. S.; Kim, Y.; Lee, K.; Choi, C.; Jung, D.; Park, C.; Heo, H.; Yang, J.; Hyeon, T.; Choi, M. K.; Kim, D.-H. Intrinsically stretchable quantum dot light-emitting diodes. *Nat. Electron.* **2024**, *7* (5), 365−374.

(14) Que, M.; Yuan, H.; Wu, Q.; He, S.; Zhong, P.; Li, B. Amino Acid Double-Passivation-Enhanced Quantum Dot Coupling for High-Efficiency $FAPbI_3$ Perovskite Quantum Dot Solar Cells. *ACS Appl. Mater.* **2024**, *16* (5), 6189−6197.

(15) Ren, J.; Opoku, H.; Tang, S.; Edman, L.; Wang, J. Carbon Dots: A Review with Focus on Sustainability. *Adv. Sci.* **2024**, No. 2405472.
(16) Shi, H.; Yin, Y.; Xu, H.; Qu, X.; Wang, H.; An, Z. Samarium doped carbon dots for near-infrared photo-therapy. *Chem. Eng. J.* **2024**, *488*, No. 150661.
(17) Yang, Y.; Sreekumar, S.; Chimenti, R. V.; Veksler, M.; Song, K.; Zhang, S.; Rodas, D.; Christianson, V.; O'Carroll, D. M. Polypropylene-Derived Luminescent Carbon Dots. *ACS Mater. Lett.* **2024**, *6* (5), 1968−1976.
(18) Yu, X.; Liu, K.; Wang, B.; Zhang, H.; Qi, Y.; Yu, J. Time-Dependent Polychrome Stereoscopic Luminescence Triggered by Resonance Energy Transfer between Carbon Dots-in-Zeolite Composites and Fluorescence Quantum Dots. *Adv. Mater.* **2023**, *35*, No. 2208735.
(19) Zhang, P.; Teng, Z.; Zhou, M.; Yu, X.; Wen, H.; Niu, J.; Liu, Z.; Zhang, Z.; Liu, Y.; Qiu, J.; Xu, X. Upconversion 3D Bioprinting for Noninvasive In Vivo Molding. *Adv. Mater.* **2024**, *36*, No. 2310617.
(20) Arshad, F.; Sk, M. P. Luminescent Sulfur Quantum Dots for Colorimetric Discrimination of Multiple Metal Ions. *ACS Appl. Nano Mater.* **2020**, *3* (3), 3044−3049.
(21) Duan, Y.; Tan, J.; Huang, Z.; Deng, Q.; Liu, S.; Wang, G.; Li, L.; Zhou, L. Facile synthesis of carboxymethyl cellulose sulfur quantum dots for live cell imaging and sensitive detection of Cr(VI) and ascorbic acid. *Carbohyd. Polym.* **2020**, *249*, No. 116882.
(22) Gao, P.; Wang, G.; Zhou, L. Cover Feature: Luminescent Sulfur Quantum Dots: Synthesis, Properties and Potential Applications (ChemPhotoChem 11/2020). *ChemPhotoChem.* **2020**, *4* (11), 5231−5231.
(23) Li, L.; Yang, C.; Li, Y.; Nie, Y.; Tian, X. Sulfur quantum dot-based portable paper sensors for fluorometric and colorimetric dual-channel detection of cobalt. *J. Mater. Sci.* **2021**, *56* (7), 4782−4796.
(24) Li, Q.-L.; Shi, L.-X.; Du, K.; Qin, Y.; Qu, S.-J.; Xia, D.-Q.; Zhou, Z.; Huang, Z.-G.; Ding, S.-N. Copper-Ion-Assisted Precipitation Etching Method for the Luminescent Enhanced Assembling of Sulfur Quantum Dots. *ACS Omega* **2020**, *5* (10), 5407−5411.
(25) Shi, Y.-e.; Zhang, P.; Yang, D.; Wang, Z. Synthesis, photoluminescence properties and sensing applications of luminescent sulfur nanodots. *Chem. Commun.* **2020**, *56* (75), 10982−10988.
(26) Ma, Q.; Zu, Y.; Guan, Y.; Ma, P.; Li, S.; Song, J.; Guo, Y. Small molecule L-cysteine assisted synthesis of green fluorescent sulfur quantum dots for nimesulide sensing and bioimaging. *Microchem. J.* **2023**, *190*, No. 108734.
(27) Mondal, A.; Pandit, S.; Sahoo, J.; Subramaniam, Y.; De, M. Post-functionalization of sulfur quantum dots and their aggregation-dependent antibacterial activity. *Nanoscale* **2023**, *15* (46), 18624−18638.
(28) Priyadarshi, R.; Pourmoslemi, S.; Khan, A.; Riahi, Z.; Rhim, J.-W. Sulfur quantum dots as sustainable materials for biomedical applications: Current trends and future perspectives. *Colloids Surf., B* **2024**, *237*, No. 113863.
(29) Wang, X.; Yan, F.; Xu, M.; Ning, J.; Wei, X.; Bai, X. Facile synthesis of multicolor emitting sulfur quantum dots and their applications in light blocking field, anti-counterfeiting and sensing. *J. Colloid Interface Sci.* **2024**, *653*, 1137−1149.
(30) Li, S.; Chen, D.; Zheng, F.; Zhou, H.; Jiang, S.; Wu, Y. Water-Soluble and Lowly Toxic Sulphur Quantum Dots. *Adv. Funct. Mater.* **2014**, *24* (45), 7133−7138.
(31) Shen, L.; Wang, H.; Liu, S.; Bai, Z.; Zhang, S.; Zhang, X.; Zhang, C. Assembling of Sulfur Quantum Dots in Fission of Sublimed Sulfur. *J. Am. Chem. Soc.* **2018**, *140* (25), 7878−7884.
(32) Wang, H.; Wang, Z.; Xiong, Y.; Kershaw, S. V.; Li, T.; Wang, Y.; Zhai, Y.; Rogach, A. L. Hydrogen Peroxide Assisted Synthesis of Highly Luminescent Sulfur Quantum Dots. *Angew. Chem., Int. Ed.* **2019**, *58* (21), 7040−7044.
(33) Song, Y.; Tan, J.; Wang, G.; Gao, P.; Lei, J.; Zhou, L. Oxygen accelerated scalable synthesis of highly fluorescent sulfur quantum dots. *Chem. Sci.* **2020**, *11* (3), 772−777.
(34) Hu, Z.; Dai, H.; Wei, X.; Su, D.; Wei, C.; Chen, Y.; Xie, F.; Zhang, W.; Guo, R.; Qu, S. 49.25% efficient cyan emissive sulfur dots via a microwave-assisted route. *RSC Adv.* **2020**, *10* (29), 17266−17269.
(35) Xiao, L.; Du, Q.; Huang, Y.; Wang, L.; Cheng, S.; Wang, Z.; Wong, T. N.; Yeow, E. K. L.; Sun, H. Rapid Synthesis of Sulfur Nanodots by One-Step Hydrothermal Reaction for Luminescence-Based Applications. *ACS Appl. Nano Mater.* **2019**, *2* (10), 6622−6628.
(36) Priyadarshi, R.; Riahi, Z.; Tammina, S. K.; Khan, A.; Rhim, J. W. Sustainable large-scale synthesis of biologically active sulfur quantum dots using sublimed sulfur. *Mater. Today Sustainability* **2023**, *24*, No. 100563.
(37) Sheng, Y.; Huang, Z.; Zhong, Q.; Deng, H.; Lai, M.; Yang, Y.; Chen, W.; Xia, X.; Peng, H. Size-focusing results in highly photoluminescent sulfur quantum dots with a stable emission wavelength. *Nanoscale* **2021**, *13* (4), 2519−2526.
(38) Li, S.; Fan, W.; Chen, Q.; Zhang, X. Facile Light-Driven Synthesis of Highly Luminous Sulfur Quantum Dots for Fluorescence Sensing and Cell Imaging. *ACS Appl. Mater.* **2024**, *16* (31), 41281−41292.
(39) Ning, K.; Fu, Y.; Wu, J.; Sun, Y.; Liu, K.; Ye, K.; Liu, J.; Wu, Y.; Liang, J. Inner filter effect-based red-shift and fluorescence dual-sensor platforms with sulfur quantum dots for detection and bioimaging of alkaline phosphatase. *Anal. Methods* **2022**, *15* (1), 79−86.
(40) Wang, C.; Wei, Z.; Pan, C.; Pan, Z.; Wang, X.; Liu, J.; Wang, H.; Huang, G.; Wang, M.; Mao, L. Dual Functional Hydrogen Peroxide Boosted One Step Solvothermal Synthesis of Highly Uniform Sulfur Quantum Dots at Elevated Temperature and Their Fluorescent Sensing. *Sens. Actuators B-Chem.* **2021**, *344*, No. 130326.
(41) Zhang, C.; Zhang, P.; Ji, X.; Wang, H.; Kuang, H.; Cao, W.; Pan, M.; Shi, Y.-e.; Wang, Z. Ultrasonication-promoted synthesis of luminescent sulfur nano-dots for cellular imaging applications. *Chem. Commun.* **2019**, *55* (86), 13004−13007.
(42) Lei, J.; Huang, Z.; Gao, P.; Sun, J.; Zhou, L. Polyvinyl Alcohol Enhanced Fluorescent Sulfur Quantum Dots for Highly Sensitive Detection of Fe^{3+} and Temperature in Cells. *Part. Part. Syst. Charact.* **2021**, *38*, No. 2000332.
(43) Qiao, G.; Liu, L.; Hao, X.; Zheng, J.; Liu, W.; Gao, J.; Zhang, C. C.; Wang, Q. Signal transduction from small particles: Sulfur nanodots featuring mercury sensing, cell entry mechanism and in vitro tracking performance. *Chem. Eng. J.* **2020**, *382*, No. 122907.
(44) Zhu, S.; Meng, Q.; Wang, L.; Zhang, J.; Song, Y.; Jin, H.; Zhang, K.; Sun, H.; Wang, H.; Yang, B. Highly Photoluminescent Carbon Dots for Multicolor Patterning, Sensors, and Bioimaging. *Angew. Chem., Int. Ed.* **2013**, *52* (14), 3953−3957.
(45) Qiu, L.; Zou, K.; Xu, G. Investigation on the sulfur state and phase transformation of spent and regenerated S zorb sorbents using XPS and XRD. *Appl. Surf. Sci.* **2013**, *266*, 230−234.
(46) Yang, C.-P.; Yin, Y.-X.; Guo, Y.-G.; Wan, L.-J. Electrochemical (De) Lithiation of 1D Sulfur Chains in Li−S Batteries: A Model System Study. *J. Am. Chem. Soc.* **2015**, *137* (6), 2215−2218.
(47) Peisert, H.; Chassé, T.; Streubel, P.; Meisel, A.; Szargan, R. Relaxation energies in XPS and XAES of solid sulfur compounds. *J. Electron Spectrosc. Relat. Phenom.* **1994**, *68*, 321−328.
(48) Cavalleri, O.; Oliveri, L.; Daccà, A.; Parodi, R.; Rolandi, R. XPS measurements on l-cysteine and 1-octadecanethiol self-assembled films: a comparative study. *Appl. Surf. Sci.* **2001**, *175*−*176*, 357−362.
(49) Dodero, G.; De Michieli, L.; Cavalleri, O.; Rolandi, R.; Oliveri, L.; Daccà, A.; Parodi, R. l-Cysteine chemisorption on gold: an XPS and STM study. *Colloids Surf. A Physicochem. Eng. Asp.* **2000**, *175* (1), 121−128.
(50) Li, F.; Li, Y.; Yang, X.; Han, X.; Jiao, Y.; Wei, T.; Yang, D.; Xu, H.; Nie, G. Highly Fluorescent Chiral N-S-Doped Carbon Dots from Cysteine: Affecting Cellular Energy Metabolism. *Angew. Chem., Int. Ed.* **2018**, *57* (9), 2377−2382.

https://doi.org/10.1021/cbmi.4c00052
Chem. Biomed. Imaging 2024, 2, 817−824